nature biotechnology

SUPPLEMENTARY INFORMATION

https://doi.org/10.1038/s41587-019-0016-3

In the format provided by the authors and unedited.

Hypoimmunogenic derivatives of induced pluripotent stem cells evade immune rejection in fully immunocompetent allogeneic recipients

Tobias Deuse[1,7], Xiaomeng Hu[1,2,3,7], Alessia Gravina[1], Dong Wang[1,2], Grigol Tediashvili[1,2,3], Chandrav De[4], William O. Thayer[4], Angela Wahl[4], J. Victor Garcia[4], Hermann Reichenspurner[2,3], Mark M. Davis[5], Lewis L. Lanier[6] and Sonja Schrepfer[1]*

[1]Department of Surgery, Division of Cardiothoracic Surgery, Transplant and Stem Cell Immunobiology-Lab, University of California San Francisco, San Francisco, CA, USA. [2]Department of Cardiovascular Surgery, University Heart Center Hamburg, Hamburg, Germany. [3]Cardiovascular Research Center Hamburg and DZHK (German Center for Cardiovascular Research), Partner Site Hamburg/Kiel/Luebeck, Hamburg, Germany. [4]Division of Infectious Diseases, UNC Center for AIDS Research, University of North Carolina School of Medicine, Chapel Hill, NC, USA. [5]Howard Hughes Medical Institute, Institute for Immunity, Transplantation and Infection, and Department of Microbiology and Immunology, Stanford University School of Medicine, Stanford, CA, USA. [6]Department of Microbiology and Immunology and the Parker Institute for Cancer Immunotherapy, University of California San Francisco, San Francisco, California, USA. [7]These authors contributed equally: Tobias Deuse, Xiaomeng Hu. *e-mail: Sonja.Schrepfer@ucsf.edu

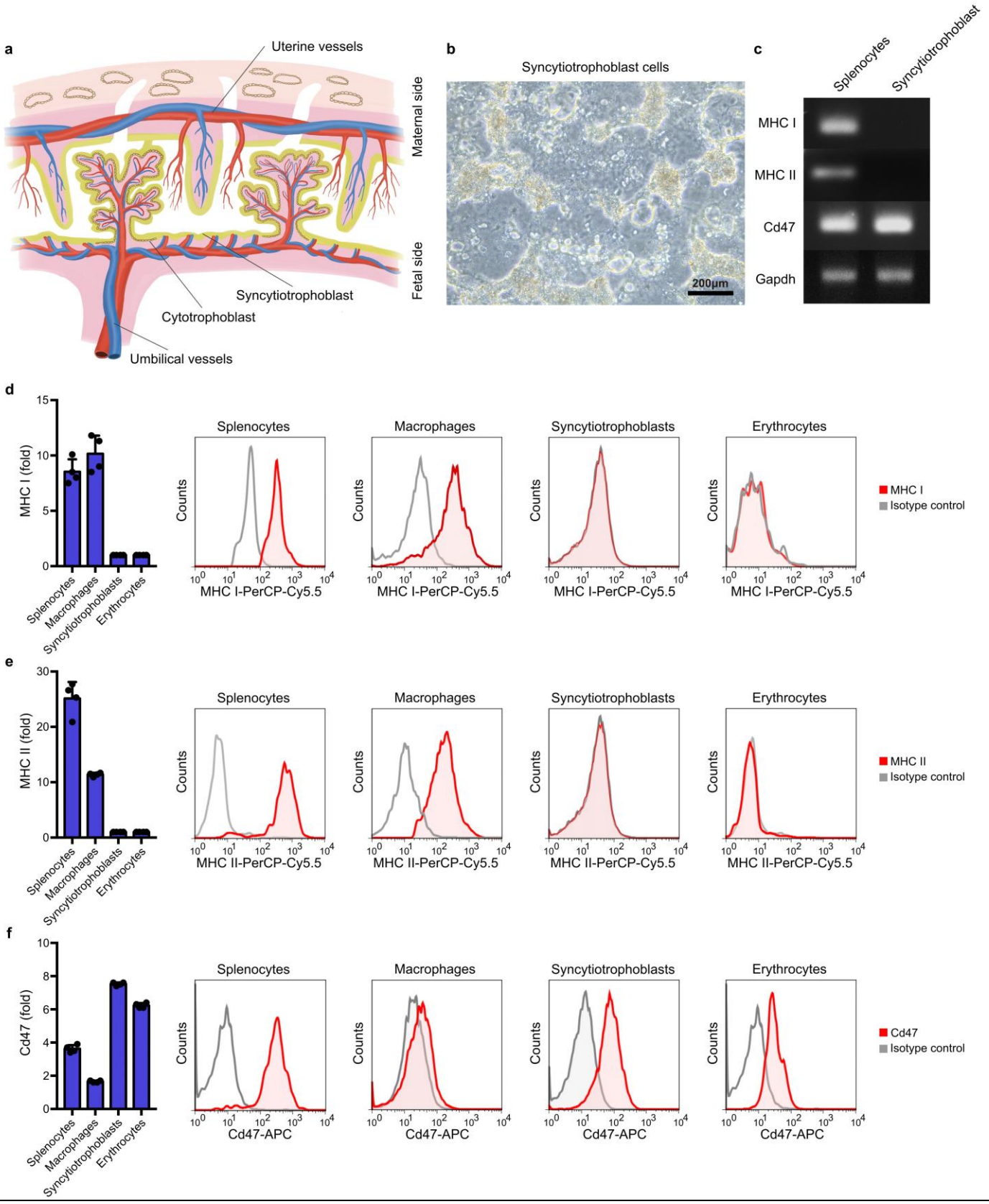
a
Uterine vessels
Maternal side
Fetal side
Syncytiotrophoblast
Cytotrophoblast
Umbilical vessels
b
Syncytiotrophoblast cells
200μm
c
Splenocytes
Syncytiotrophoblast
MHC I
MHC II
Cd47
Gapdh
d
MHC I (fold)
Splenocytes
Macrophages
Syncytiotrophoblasts
Erythrocytes
Counts
MHC I-PerCP-Cy5.5
MHC I
Isotype control
e
MHC II (fold)
MHC II-PerCP-Cy5.5
MHC II
Isotype control
f
Cd47 (fold)
Cd47-APC
Cd47
Isotype control

Supplementary Figure 1

The immune phenotype of syncytiotrophoblast cells.

a, The syncytiotrophoblast is the immediate interface between maternal blood and the fetal side of the placenta. **b**, Mouse syncytiotrophoblast cells were isolated and cultured (representative picture of two independent experiments). **c**, RT-PCR showed depleted MHC class I and II expression, but positive Cd47 expression (representative gel of three independent experiments). **d-f**, The surface expression of MHC class I (d), MHC class II (e), and Cd47 (f) was assessed by flow cytometry (mean ±s.d., 4 independent experiments per group). Representative histograms are shown.

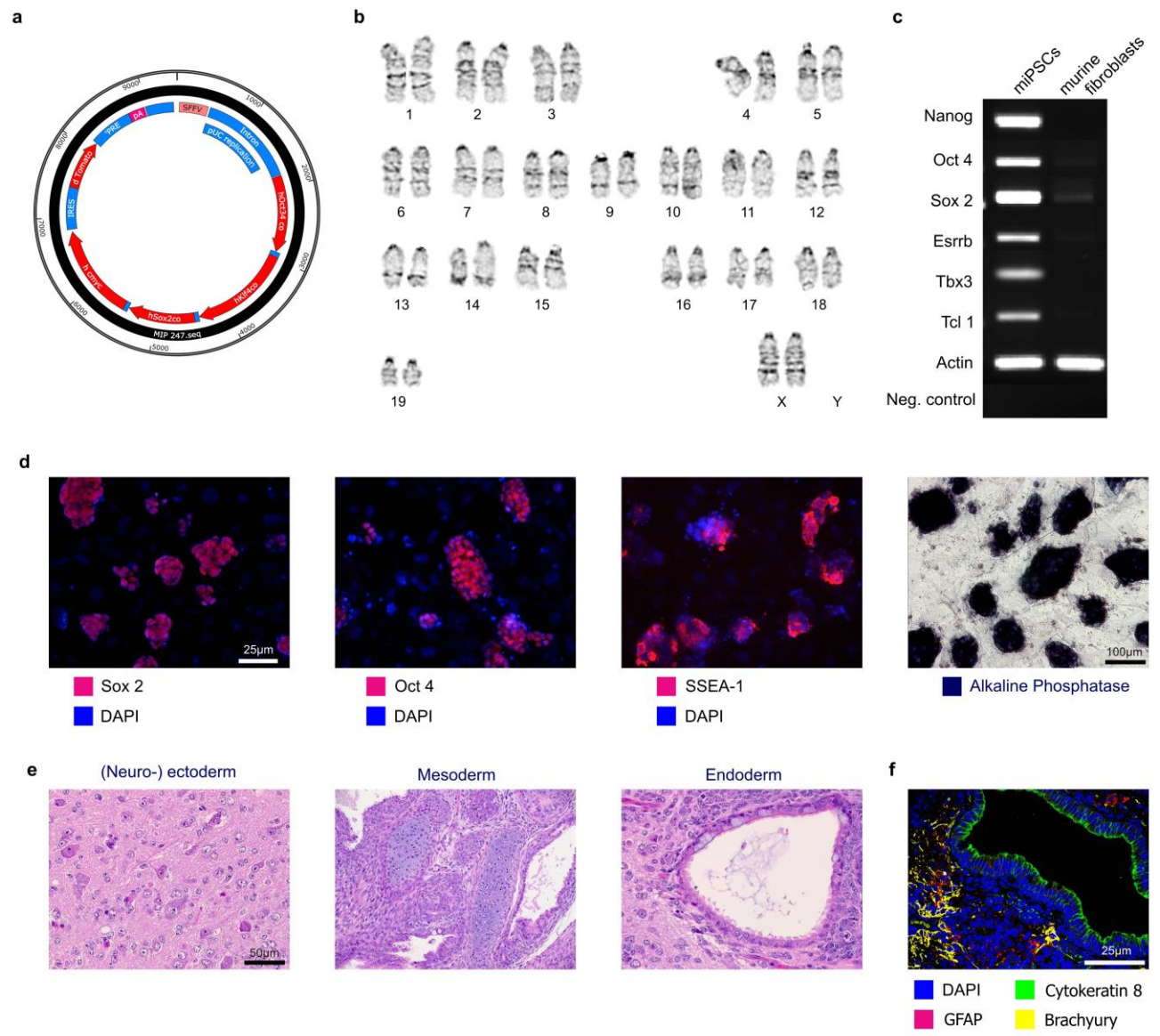

Supplementary Figure 2

The generation of miPSCs.

a, Mouse tail tip fibroblasts were re-programmed using a plasmid expressing the four re-programming factors Oct4, KLF4, Sox2, and c-Myc. **b**, The miPSCs showed a normal 40, XX mouse karyotype in one analysis. **c**, miPSCs showed the typical gene expression profile of pluripotent stem cells (representative gel of two independent experiments). **d**, In immunofluorescence, miPSC cultures were positive for Sox2, Oct4, SSEA-1, and alkaline phosphatase (representative pictures of three independent experiments). **e**, When transplanted into immunodeficient SCID-beige mice, they formed teratomas containing (neuro-) ectoderm, mesoderm, and endoderm (representative pictures of three independent experiments). **f**, Endodermal (cytokeratin 8), mesodermal (brachyury), and ectodermal (GFAP) lineages were demonstrated by confocal immunofluorescence microscopy (representative pictures of three independent experiments).

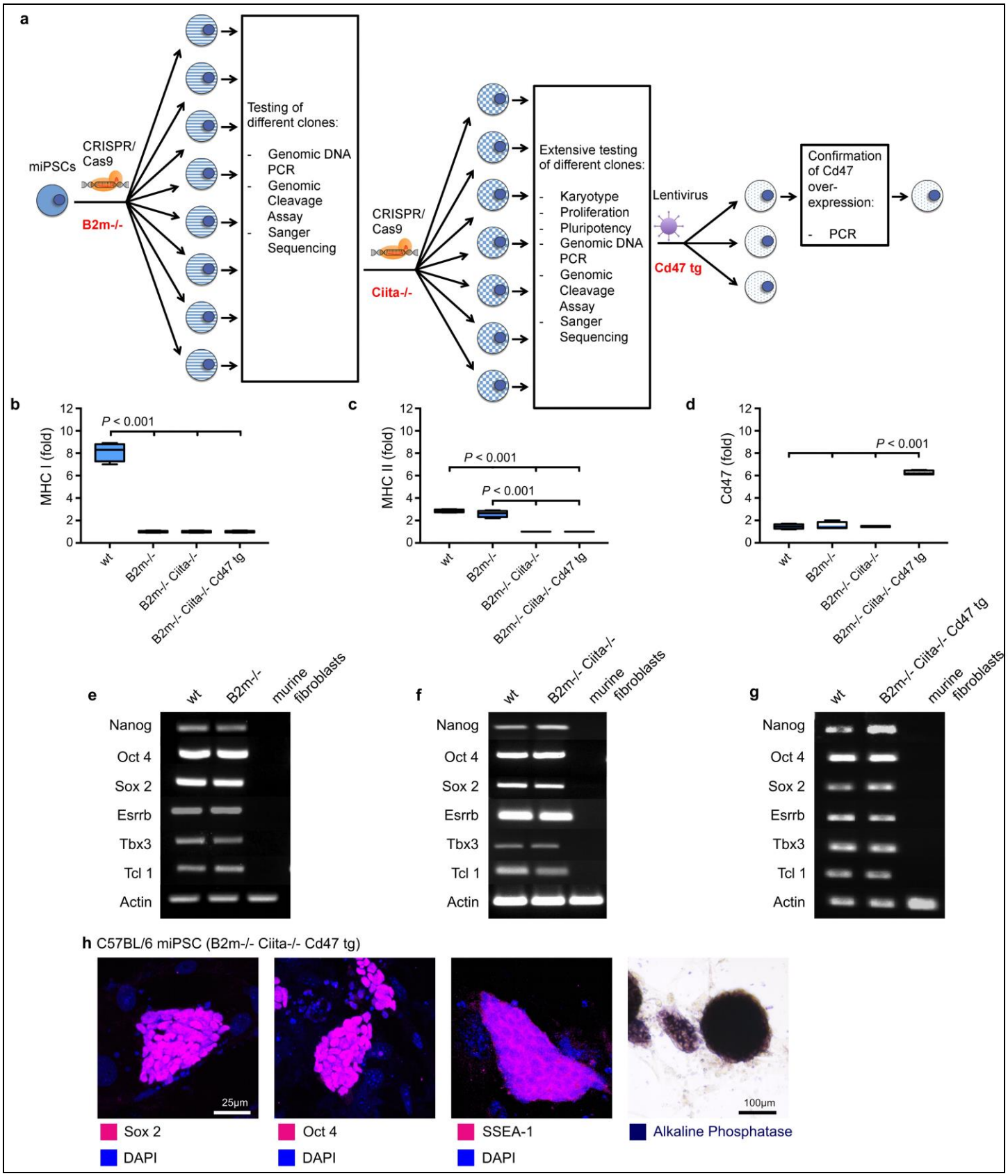
a
miPSCs
CRISPR/
Cas9
B2m-/-
Testing of different clones:
- Genomic DNA PCR
- Genomic Cleavage Assay
- Sanger Sequencing
CRISPR/
Cas9
Ciita-/-
Extensive testing of different clones:
- Karyotype
- Proliferation
- Pluripotency
- Genomic DNA PCR
- Genomic Cleavage Assay
- Sanger Sequencing
Lentivirus
Cd47 tg
Confirmation of Cd47 over-expression:
- PCR
b
MHC I (fold)
P < 0.001
wt
B2m-/-
B2m-/- Ciita-/-
B2m-/- Ciita-/- Cd47 tg
c
MHC II (fold)
P < 0.001
P < 0.001
d
Cd47 (fold)
P < 0.001
e
wt
B2m-/-
murine fibroblasts
Nanog
Oct 4
Sox 2
Esrrb
Tbx3
Tcl 1
Actin
f
wt
B2m-/- Ciita-/-
murine fibroblasts
g
wt
B2m-/- Ciita-/- Cd47 tg
murine fibroblasts
h C57BL/6 miPSC (B2m-/- Ciita-/- Cd47 tg)
25µm
100µm
Sox 2
DAPI
Oct 4
DAPI
SSEA-1
DAPI
Alkaline Phosphatase

Supplementary Figure 3

Immune phenotype and pluripotency of engineered miPSCs.

a, Mouse iPSCs underwent three editing steps to disrupt *B2m*, *Ciita*, and over-express Cd47 to achieve a hypo-immunogenic phenotype. Every step included rigorous testing for quality control. **b-d**, MHC class I (b), MHC class II (c), and Cd47 expression (d) by flow cytometry is shown for each engineering step, confirming successful gene editing (box 25th to 75th percentile with median, whiskers min-max, 4 independent experiments per graph, ANOVA with Bonferroni's post-hoc test). **e-g**, During the engineering process, all edited miPSCs maintained expression of the pluripotent gene expression signature (representative gel of two independent PCR experiments). **h**, *B2m*$^{-/-}$*Ciita*$^{-/-}$ Cd47 tg miPSCs exhibited Sox2, Oct4, and SSEA-1 expression in confocal immunofluorescence stainings, as well as alkaline phosphatase in immunohistochemistry (representative pictures of three independent experiments).

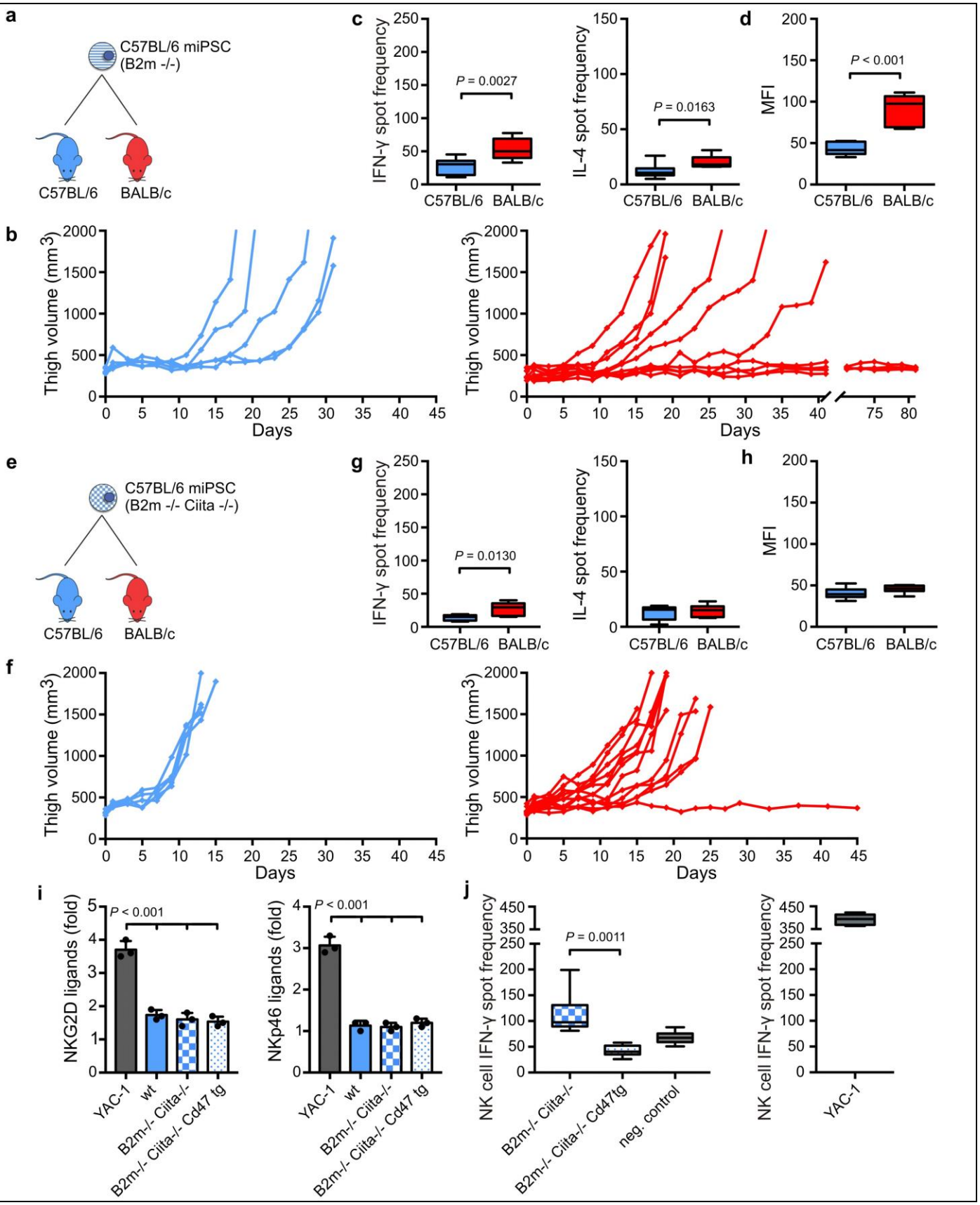
a
C57BL/6 miPSC
(B2m -/-)
C57BL/6
BALB/c
c
IFN-γ spot frequency
P = 0.0027
C57BL/6
BALB/c
IL-4 spot frequency
P = 0.0163
C57BL/6
BALB/c
d
MFI
P < 0.001
C57BL/6
BALB/c
b
Thigh volume (mm3)
Days
Thigh volume (mm3)
Days
e
C57BL/6 miPSC
(B2m -/- Ciita -/-)
C57BL/6
BALB/c
g
IFN-γ spot frequency
P = 0.0130
C57BL/6
BALB/c
IL-4 spot frequency
C57BL/6
BALB/c
h
MFI
C57BL/6
BALB/c
f
Thigh volume (mm3)
Days
Thigh volume (mm3)
Days
i
NKG2D ligands (fold)
P < 0.001
YAC-1
wt
B2m-/- Ciita-/-
B2m-/- Ciita-/- Cd47 tg
NKp46 ligands (fold)
P < 0.001
YAC-1
wt
B2m-/- Ciita-/-
B2m-/- Ciita-/- Cd47 tg
j
NK cell IFN-γ spot frequency
P = 0.0011
B2m-/- Ciita-/-
B2m-/- Ciita-/- Cd47tg
neg. control
NK cell IFN-γ spot frequency
YAC-1

Supplementary Figure 4

Survival of gene-engineered miPSCs.

a, C57BL/6 *B2m*$^{-/-}$ miPSCs were transplanted into either syngeneic C57BL/6 (blue) mice or allogeneic (red) BALB/c mice. **b,** The thigh volume of all five C57BL/6 and ten BALB/c animals is shown over time. The overall percentage of cell grafts that survived and formed teratomas in BALB/c was 60%. **c**, IFN-γ Elispots and IL-4 Elispots are shown with splenocytes recovered 5 days after the transplantation and *B2m*$^{-/-}$ miPSCs stimulator cells (box 25th to 75th percentile with median, whiskers min-max, 8 animals per group, two-tailed Student's t-test). **d**, Mean fluorescence (MFI) of IgM binding to *B2m*$^{-/-}$ miPSCs incubated with recipient serum after 5 days (box 25th to 75th percentile with median, whiskers min-max, 6 animals per group, two-tailed Student's t-test). **e**, C57BL/6 *B2m*$^{-/-}$*Ciita*$^{-/-}$ miPSCs were transplanted into syngeneic C57BL/6 or allogeneic BALB/c mice. **f**, The thigh volume of all 5 C57BL/6 and 12 BALB/c animals is shown over time. The overall percentage of cell grafts that survived and formed teratomas in BALB/c was 91.7%. **g**, IFN-γ Elispots and IL-4 Elispots are shown with splenocytes recovered 5 days after the transplantation and *B2m*$^{-/-}$*Ciita*$^{-/-}$ miPSCs stimulator cells (box 25th to 75th percentile with median, whiskers min-max, 6 animals per group, two-tailed Student's t-test). **h**, Mean fluorescence (MFI) of IgM binding to *B2m*$^{-/-}$*Ciita*$^{-/-}$ miPSCs incubated with recipient serum after 5 days (box 25th to 75th percentile with median, whiskers min-max, 6 animals per group, two-tailed Student's t-test). **i**, The expression of stimulatory NKG2D ligands and NKp46 ligands on miPSC lines and YAC-1 was assessed using receptor Fc chimera proteins in flow cytometry (mean ± s.d., 3 independent experiments per group, ANOVA with Bonferroni's post-hoc test). **j**, IFN-γ spot frequencies of miPSC lines and YAC-1 in Elispot assays with BALB/c NK cells (box 25th to 75th percentile with median, whiskers min-max, 6 independent experiments, ANOVA with Bonferroni's post-hoc test).

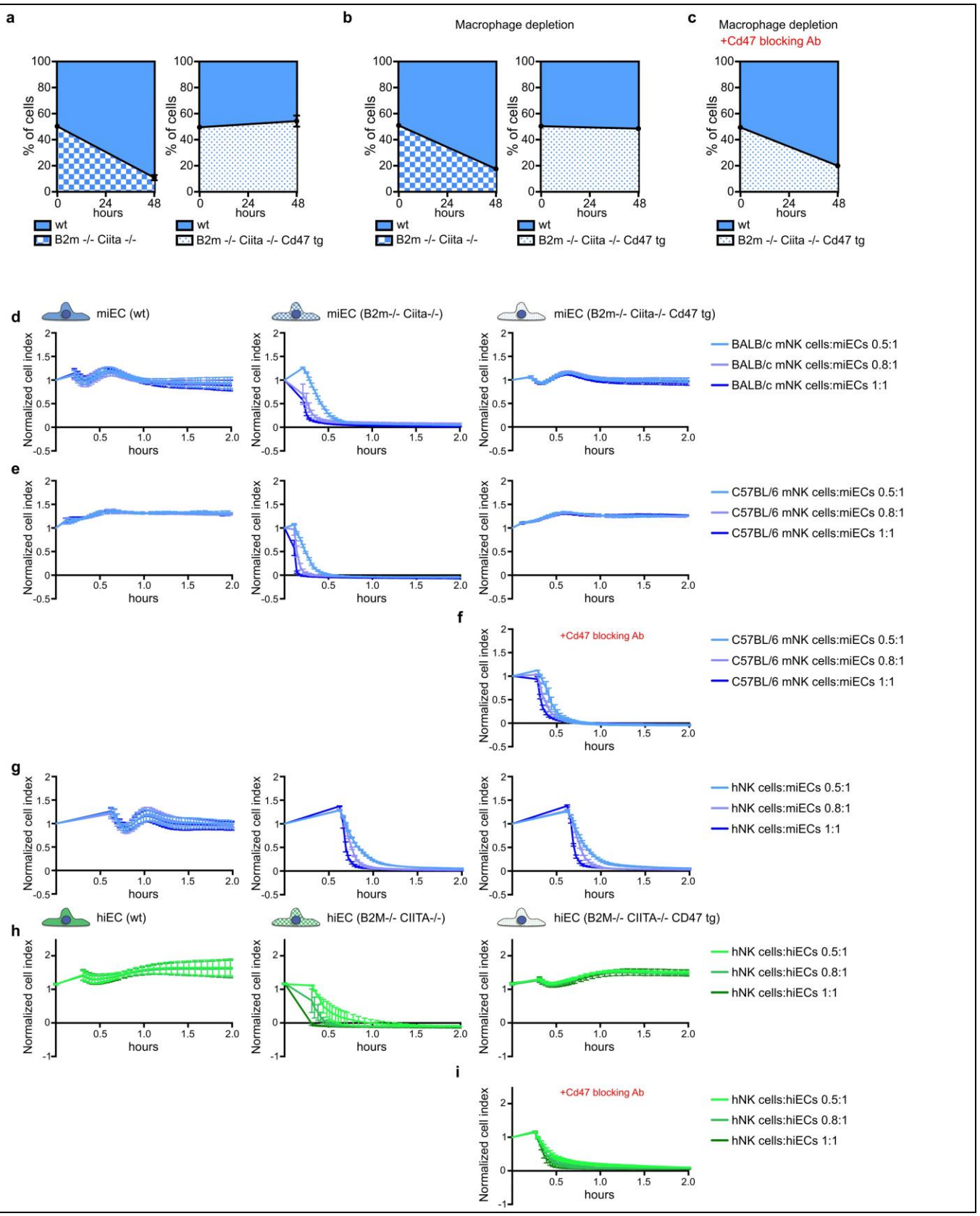
a
b
c
Macrophage depletion
Macrophage depletion
+Cd47 blocking Ab
% of cells
hours
wt
B2m -/- Ciita -/-
B2m -/- Ciita -/- Cd47 tg
d
miEC (wt)
miEC (B2m-/- Ciita-/-)
miEC (B2m-/- Ciita-/- Cd47 tg)
Normalized cell index
BALB/c mNK cells:miECs 0.5:1
BALB/c mNK cells:miECs 0.8:1
BALB/c mNK cells:miECs 1:1
e
C57BL/6 mNK cells:miECs 0.5:1
C57BL/6 mNK cells:miECs 0.8:1
C57BL/6 mNK cells:miECs 1:1
f
+Cd47 blocking Ab
C57BL/6 mNK cells:miECs 0.5:1
C57BL/6 mNK cells:miECs 0.8:1
C57BL/6 mNK cells:miECs 1:1
g
hNK cells:miECs 0.5:1
hNK cells:miECs 0.8:1
hNK cells:miECs 1:1
h
hiEC (wt)
hiEC (B2M-/- CIITA-/-)
hiEC (B2M-/- CIITA-/- CD47 tg)
hNK cells:hiECs 0.5:1
hNK cells:hiECs 0.8:1
hNK cells:hiECs 1:1
i
+Cd47 blocking Ab
hNK cells:hiECs 0.5:1
hNK cells:hiECs 0.8:1
hNK cells:hiECs 1:1

Supplementary Figure 5

Interaction between CD47 and NK cells.

a, *In vivo* innate immune clearance was assessed by injecting a 1 : 1 mixture of CFSE-labeled wt miPSCs and either *B2m*$^{-/-}$*Ciita*$^{-/-}$ or *B2m*$^{-/-}$*Ciita*$^{-/-}$ Cd47 tg miPSCs into the peritoneum of syngeneic C57BL/6 mice. After 48 h, CSFE-labeled peritoneal miPSCs were recovered and the percentages of both fractions assessed by flow cytometry (mean ± s.d., 4 animals per group). While *B2m*$^{-/-}$*Ciita*$^{-/-}$ miPSCs were rapidly cleared, *B2m*$^{-/-}$*Ciita*$^{-/-}$ Cd47 tg miPSCs were spared. **b**, Mice were pre-treated with clodronate to deplete macrophages, making this model more specific to NK cell killing and again only *B2m*$^{-/-}$*Ciita*$^{-/-}$ Cd47 tg miPSCs were spared from NK cell killing (mean ± s.d., 4 animals per group). **c**, When a Cd47 blocking antibody was co-injected into the peritoneum, the protection was abolished and *B2m*$^{-/-}$*Ciita*$^{-/-}$ Cd47 tg miPSCs were killed (mean ± s.d., 4 animals per group). **d**, *In vitro* real-time NK cell killing was assessed on confluent wt, *B2m*$^{-/-}$*Ciita*$^{-/-}$, and *B2m*$^{-/-}$*Ciita*$^{-/-}$ Cd47 tg miECs in three different effector : target cell ratios. Using allogeneic BALB/c mouse NK (mNK) cells, *B2m*$^{-/-}$*Ciita*$^{-/-}$ miECs were rapidly killed, and wt and *B2m*$^{-/-}$*Ciita*$^{-/-}$ Cd47 tg miECs permanently survived (mean ± s.d., 3 independent experiments per group). **e**, Similarly, using syngeneic C57BL/6 mNK cells, *B2m*$^{-/-}$*Ciita*$^{-/-}$ miECs were rapidly killed, and wt and *B2m*$^{-/-}$*Ciita*$^{-/-}$ Cd47 tg miECs permanently survived (mean ± s.d., 3 independent experiments per group). **f**, When a Cd47 blocking antibody was added to syngeneic C57BL/6 mNK cells, *B2m*$^{-/-}$*Ciita*$^{-/-}$ Cd47 tg miECs were swiftly killed (mean ± s.d., 3 independent experiments per group). **g**, When human NK (hNK) cells were used, both *B2m*$^{-/-}$*Ciita*$^{-/-}$ and *B2m*$^{-/-}$*Ciita*$^{-/-}$ Cd47 tg miECs were rapidly killed (mean ± s.d., 3 independent experiments per group). **h**, When hNK cells were used with human wt, *B2M*$^{-/-}$*CIITA*$^{-/-}$, and *B2M*$^{-/-}$*CIITA*$^{-/-}$ CD47 tg hiECs, only *B2M*$^{-/-}$*CIITA*$^{-/-}$ hiECs were rapidly killed and wt and *B2M*$^{-/-}$*CIITA*$^{-/-}$ CD47 tg hiECs were spared (mean ± s.d., 3 independent experiments per group). **i**, With a CD47 blocking antibody, *B2M*$^{-/-}$*CIITA*$^{-/-}$ CD47 tg hiECs were then swiftly killed (mean ± s.d., 3 independent experiments per group).

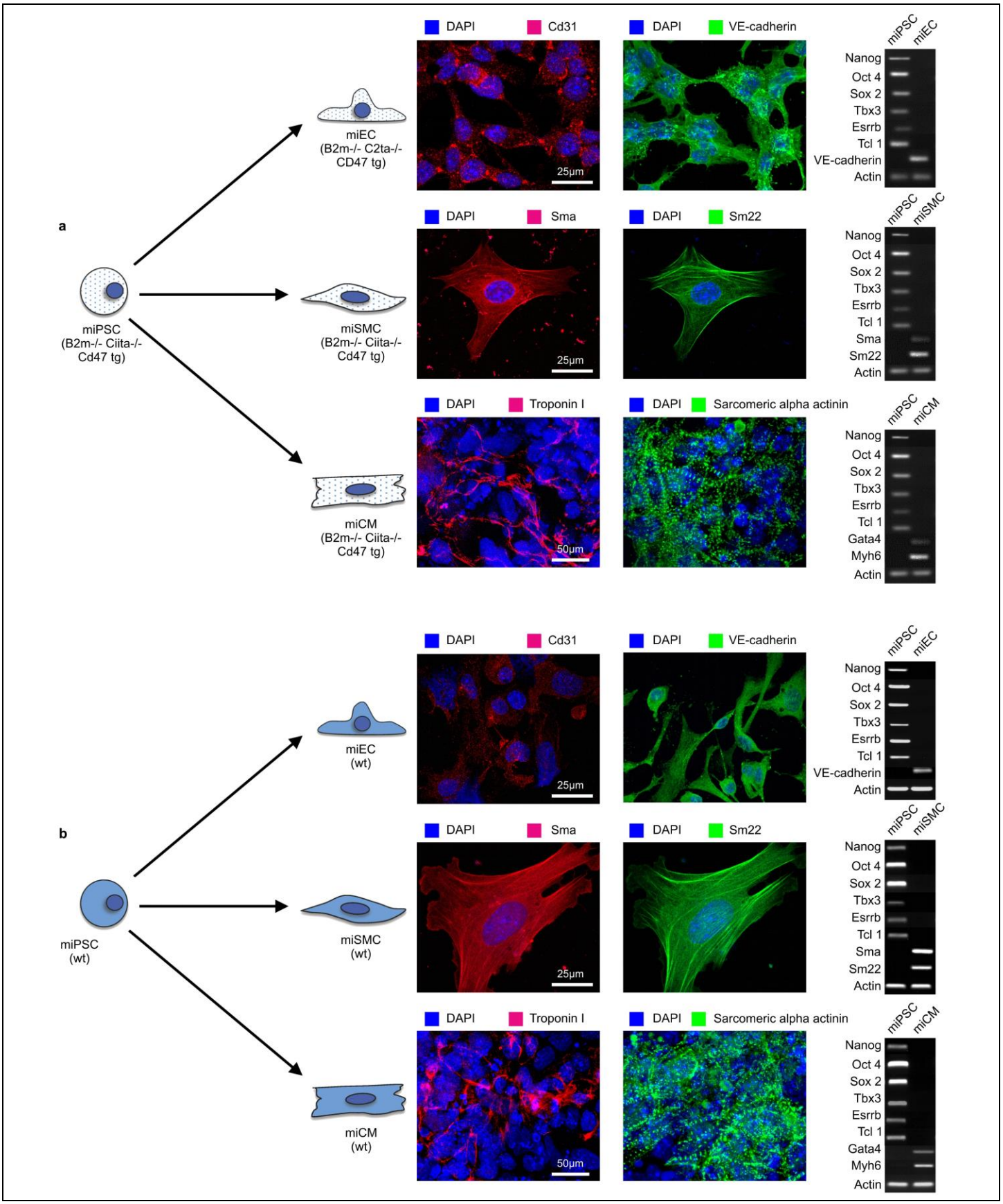
a
miPSC
(B2m-/- Ciita-/-
Cd47 tg)
miEC
(B2m-/- C2ta-/-
CD47 tg)
miSMC
(B2m-/- Ciita-/-
Cd47 tg)
miCM
(B2m-/- Ciita-/-
Cd47 tg)
DAPI
Cd31
DAPI
VE-cadherin
25µm
DAPI
Sma
DAPI
Sm22
25µm
DAPI
Troponin I
DAPI
Sarcomeric alpha actinin
50µm
miPSC
miEC
miSMC
miCM
Nanog
Oct 4
Sox 2
Tbx3
Esrrb
Tcl 1
VE-cadherin
Sma
Sm22
Gata4
Myh6
Actin
b
miPSC
(wt)
miEC
(wt)
miSMC
(wt)
miCM
(wt)
DAPI
Cd31
DAPI
VE-cadherin
25µm
DAPI
Sma
DAPI
Sm22
25µm
DAPI
Troponin I
DAPI
Sarcomeric alpha actinin
50µm
miPSC
miEC
miSMC
miCM
Nanog
Oct 4
Sox 2
Tbx3
Esrrb
Tcl 1
VE-cadherin
Sma
Sm22
Gata4
Myh6
Actin

Supplementary Figure 6
Differentiation of miPSCs into miECs, miSMCs and miCMs.
a-b, *B2m*$^{-/-}$*Ciita*$^{-/-}$ Cd47 tg miPSCs (a) and wt miPSCs (b) were successfully differentiated into corresponding miEC, miSMC, and miCM derivatives (representative pictures of three independent experiments). miECs were positive for Cd31 and VE-cadherin, miSMCs were positive for Sma and Sm22, miCMs were positive for Troponin I and Sarcomeric alpha-actinin by confocal immunofluorescence. All derivatives lost their expression of pluripotency genes (representative pictures of two independent PCR experiments).

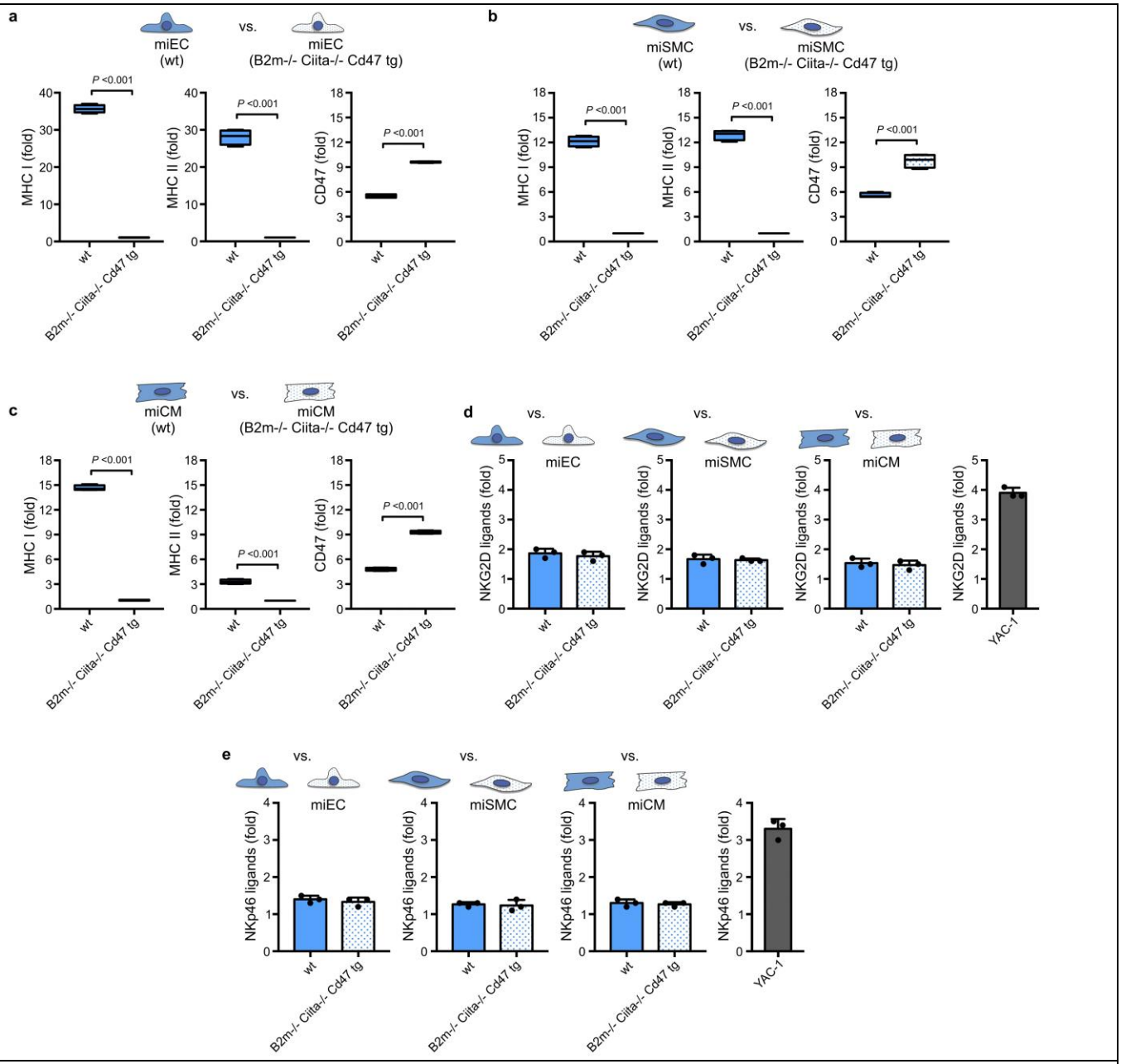

Supplementary Figure 7

Immune phenotype of wt and engineered miPSC derivatives.

a, wt miECs showed high MHC class I and MHC class II expression, while *B2m*$^{-/-}$*Ciita*$^{-/-}$ Cd47 tg miECs were MHC class I and MHC class II depleted and showed increased Cd47 expression (box 25th to 75th percentile with median, whiskers min-max, 4 independent experiments per graph, two-tailed Student's t-test). **b**, wt miSMCs showed moderate MHC class I and MHC class II expression, while *B2m*$^{-/-}$*Ciita*$^{-/-}$ Cd47 tg miSMCs were MHC class I and MHC class II depleted and showed increased Cd47 expression (box 25th to 75th percentile with median, whiskers min-max, 4 independent experiments per graph, two-tailed Student's t-test). **c**, wt miCMs showed moderate MHC class I and low MHC class II expression; *B2m*$^{-/-}$*Ciita*$^{-/-}$ Cd47 tg miCMs were MHC class I and MHC class II depleted and showed increased Cd47 expression (box 25th to 75th percentile with median, whiskers min-max, 4 independent experiments per graph, two-tailed Student's t-test). **d-e**, The expression of stimulatory NKG2D ligands (d) and NKp46 ligands (e) on wt and *B2m*$^{-/-}$*Ciita*$^{-/-}$ Cd47 tg miECs, miSMCs, miCMs, and YAC-1 was assessed using receptor Fc chimera proteins in flow cytometry (mean ± s.d., 3 independent experiments per group, two-tailed Student's t-test).

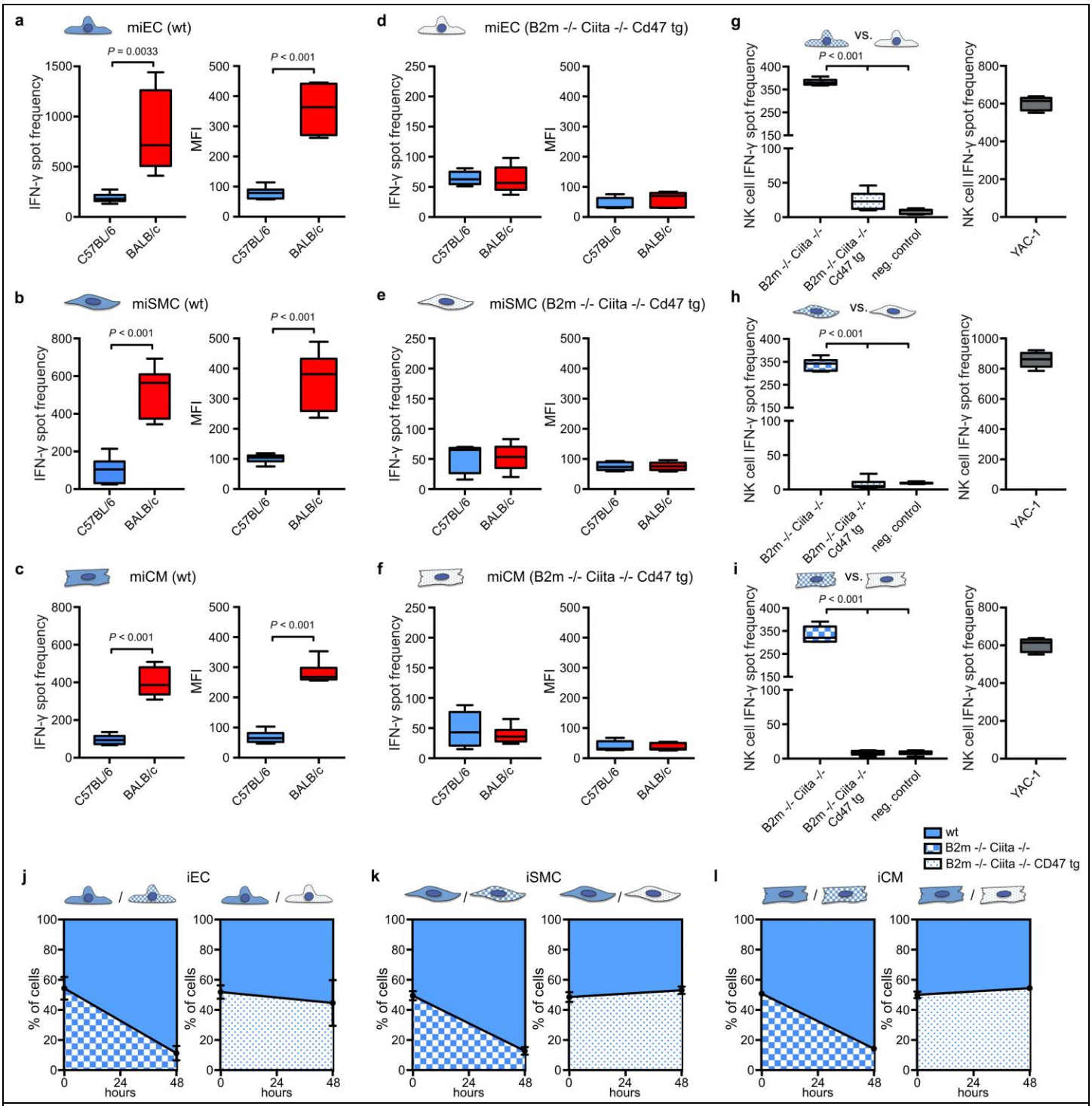

Supplementary Figure 8

Immune response against miPSC derivatives.

a-c, Five days after the injection of wt miPSC-derived miECs (a), miSMCs (b), or miCMs (c) into C57BL/6 or BALB/c recipients, splenocytes were recovered for IFN-γ Elispot assays (box 25th to 75th percentile with median, whiskers min-max, 6 animals per group, two-tailed Student's t-test). The IFN-γ response was vastly stronger in all allogeneic recipients. Mean fluorescence (MFI) of IgM binding to wt miPSC-derived miECs (a), miSMCs (b), and miCMs (c), incubated with recipient serum after 5 days (box 25th to 75th percentile

with median, whiskers min-max, 6 animals per group, two-tailed Student's t-test). There was a markedly stronger IgM response in all allogeneic recipients. **d-f**, Similarly, *B2m*$^{-/-}$*Ciita*$^{-/-}$ Cd47 tg miPSC-derived miECs (d), miSMCs (e), or miCMs (f) were injected into C57BL/6 or BALB/c recipients and IFN-γ Elispots were performed after 5 days (box 25th to 75th percentile with median, whiskers min-max, 6 animals per group, two-tailed Student's t-test). Mean fluorescence (MFI) of IgM binding to *B2m*$^{-/-}$*Ciita*$^{-/-}$ Cd47 tg miPSC-derived miECs (d), miSMCs (e), and miCMs (f), incubated with recipient serum after 5 days (box 25th to 75th percentile with median, whiskers min-max, 6 animals per group, two-tailed Student's t-test). There was no measurable IFN-γ response or IgM response in allogeneic recipients. **g-i**, To assess the inhibitory effect of Cd47 over-expression on NK cell killing, IFN-γ Elispots with NK cells were performed with miECs (g), miSMCs (h), or miCMs (i) derived from *B2m*$^{-/-}$*Ciita*$^{-/-}$ miPSC or *B2m*$^{-/-}$*Ciita*$^{-/-}$ Cd47 tg miPSC (box 25th to 75th percentile with median, whiskers min-max, 6 independent experiments, ANOVA with Bonferroni's post-hoc test) Only derivatives from *B2m*$^{-/-}$*Ciita*$^{-/-}$ miPSC were susceptible for NK cell killing. **j-l**, *In vivo* innate immune clearance was assessed by injecting a 1 : 1 mixture of wt derivative engineered derivative into the peritoneum of C57BL/6 mice. After 48 h, peritoneal miECs (j), miSMCs (k), and miCMs (l) were recovered and the percentage assessed by flow cytometry (mean ± s.d., 4 animals per group).

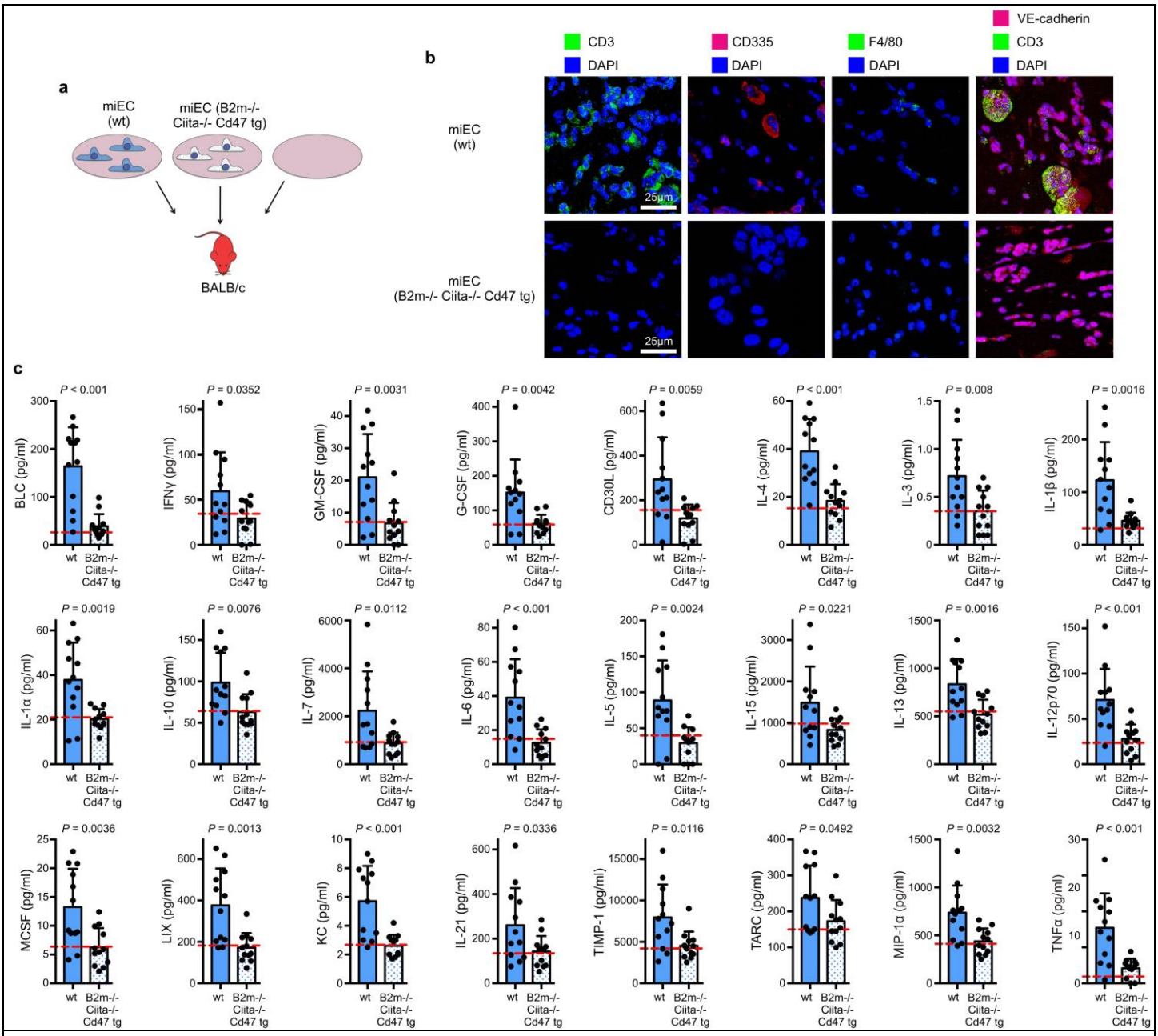

Supplementary Figure 9

Immune cell infiltration and cytokine expression in miEC grafts.

a, Matrigel plugs containing either wt miECs or *B2m*$^{-/-}$*Ciita*$^{-/-}$ Cd47 tg miECs were implanted in allogeneic BALB/c recipients. Cell-free matrigel plugs served as controls. **b**, Immunofluorescence stainings detected immune cell infiltration in wt iEC-plaques containing CD3^{+} T lymphocytes, CD335^{+} NK cells, and sparse F4/80^{+} macrophages. Co-staining of CD3 and VE-cadherin confirmed CD3^{+} lymphocyte infiltration in EC grafts in the wt group. Practically no immune cells were found in plugs containing *B2m*$^{-/-}$*Ciita*$^{-/-}$ Cd47 tg miECs (representative pictures of three independent experiments). **c**, The cytokine profile in wt miEC plugs was shifted towards a pro-inflammatory milieu. Multiple significantly up-regulated cytokines were typical of activated cytotoxic CD8^{+} T cells, CD4^{+} T helper-1 cells, and CD4^{+} T helper-2 cells, as well as macrophages (mean ± s.d., 12 animals per group, two-tailed Student's t-test; dashed red lines show levels of cell-free matrigel).

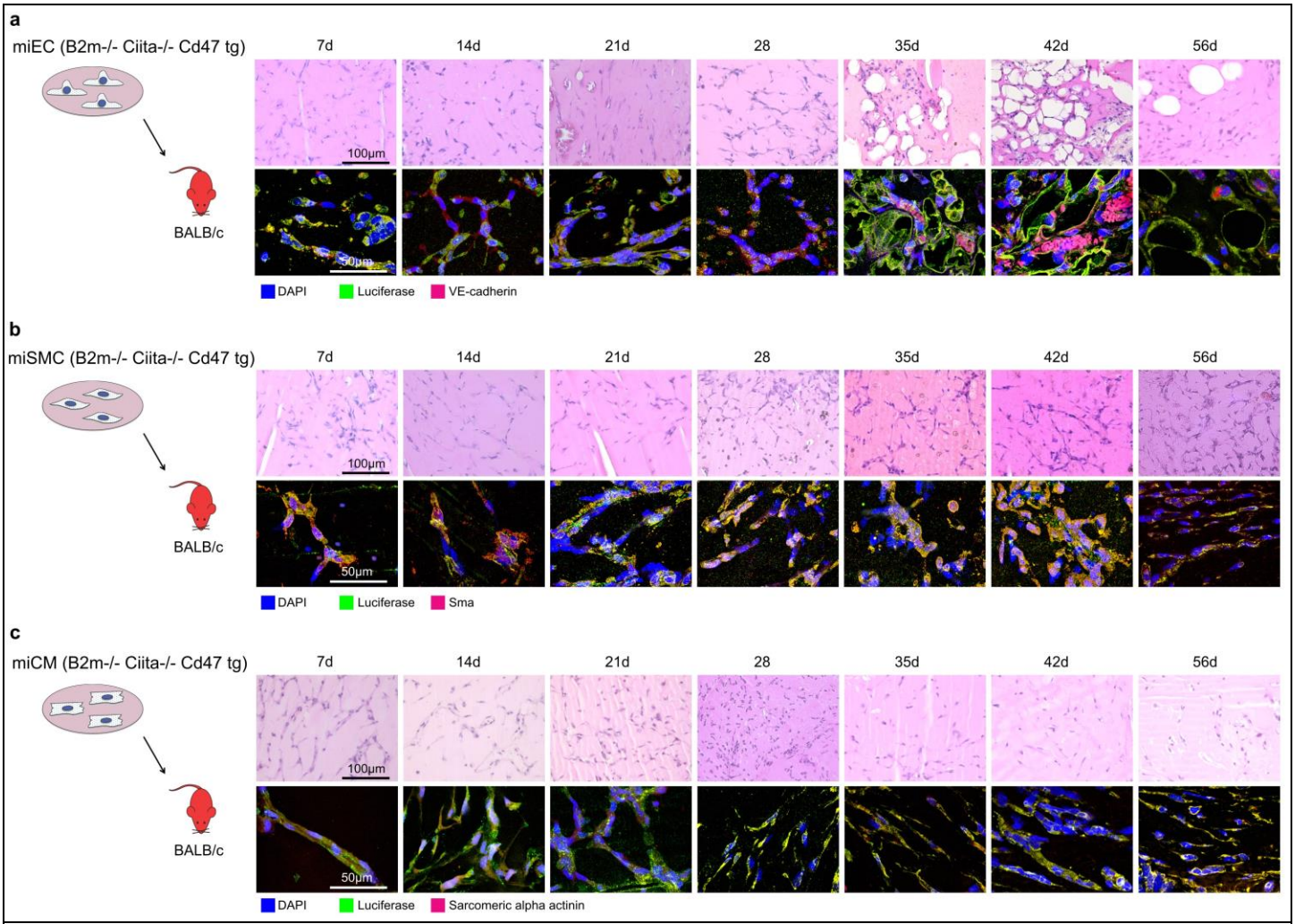

Supplementary Figure 10

Morphology of transplanted *B2m*$^{-/-}$*Ciita*$^{-/-}$ Cd47 tg miPSC derivatives in allogeneic hosts.

a-c, *B2m*$^{-/-}$*Ciita*$^{-/-}$ Cd47 tg miEC (a), miSMC (b), or miCM (c) grafts in matrigel were transplanted subcutaneously into allogeneic BALB/c mice to investigate whether these hypo-immunogenic derivatives further mature *in vivo* or change their morphology over time in allogeneic recipients. Matrigel plugs were recovered after different time points for hematoxylin and eosin and immunofluorescence stainings (representative pictures of two independent experiments). Transplanted miECs started to organize in circular structures around day 14 and formed primitive vessels that contained erythrocytes around day 35 (a). Transplanted miSMCs (b) maintained their typical spindle-shape appearance and loose arrangement, whereas miCMs retained their immature round progenitor morphology (c). Both latter cell types did not show a higher degree of three-dimensional organization, which may be attributed to the lack of mechanical stimulus necessary for maturation of any type of muscle cell.

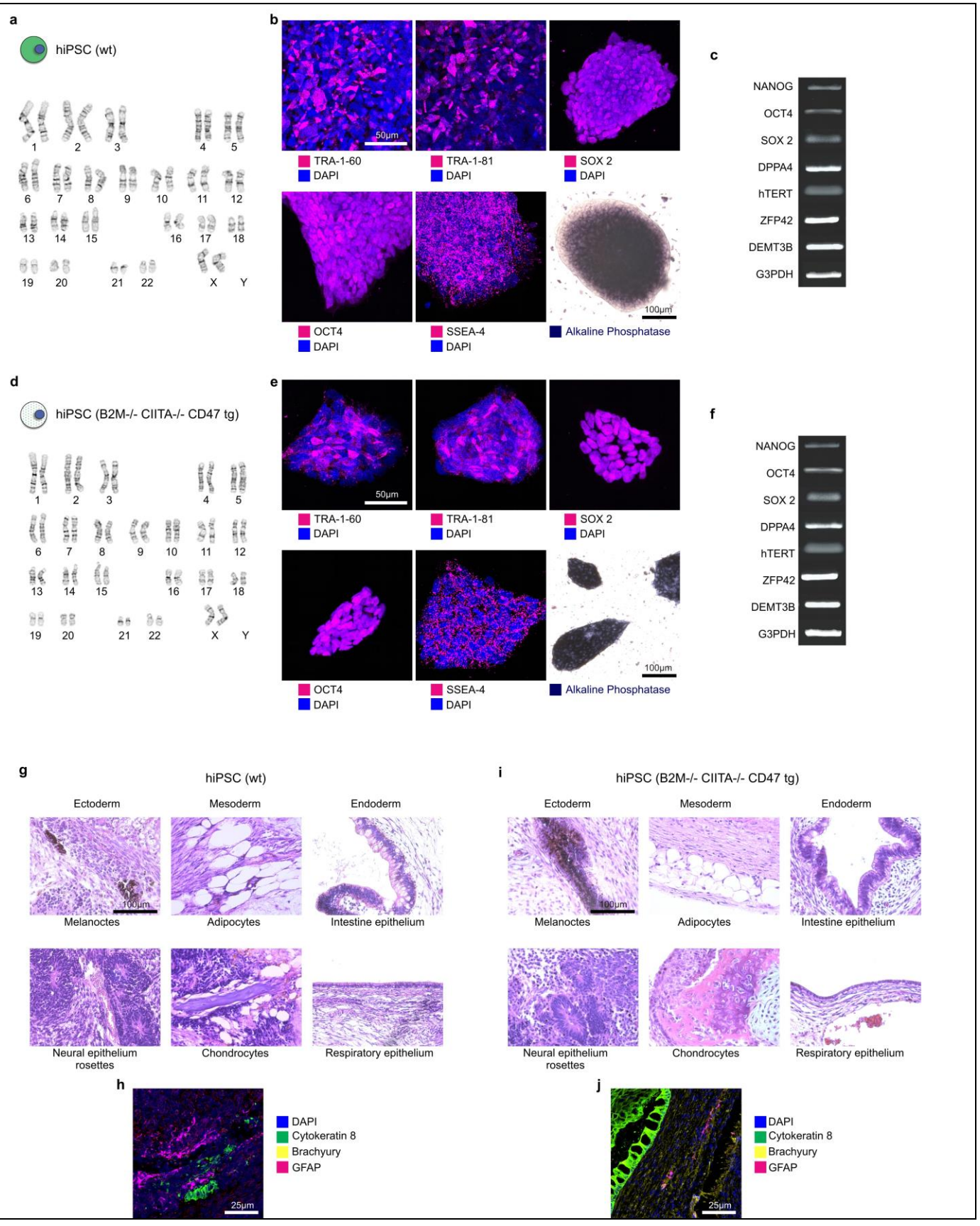
a
hiPSC (wt)
1 2 3 4 5
6 7 8 9 10 11 12
13 14 15 16 17 18
19 20 21 22 X Y
b
50μm
TRA-1-60
DAPI
TRA-1-81
DAPI
SOX 2
DAPI
OCT4
DAPI
SSEA-4
DAPI
100μm
Alkaline Phosphatase
c
NANOG
OCT4
SOX 2
DPPA4
hTERT
ZFP42
DEMT3B
G3PDH
d
hiPSC (B2M-/- CIITA-/- CD47 tg)
1 2 3 4 5
6 7 8 9 10 11 12
13 14 15 16 17 18
19 20 21 22 X Y
e
50μm
TRA-1-60
DAPI
TRA-1-81
DAPI
SOX 2
DAPI
OCT4
DAPI
SSEA-4
DAPI
100μm
Alkaline Phosphatase
f
NANOG
OCT4
SOX 2
DPPA4
hTERT
ZFP42
DEMT3B
G3PDH
g
hiPSC (wt)
Ectoderm
Mesoderm
Endoderm
100μm
Melanoctes
Adipocytes
Intestine epithelium
Neural epithelium rosettes
Chondrocytes
Respiratory epithelium
i
hiPSC (B2M-/- CIITA-/- CD47 tg)
Ectoderm
Mesoderm
Endoderm
100μm
Melanoctes
Adipocytes
Intestine epithelium
Neural epithelium rosettes
Chondrocytes
Respiratory epithelium
h
25μm
DAPI
Cytokeratin 8
Brachyury
GFAP
j
25μm
DAPI
Cytokeratin 8
Brachyury
GFAP

Supplementary Figure 11

Pluripotency of wt and *B2M*$^{-/-}$*CIITA*$^{-/-}$ CD47 tg hiPSCs.

a, wt hiPSCs showed a normal human 46, XX karyotype in one analysis. **b**, wt hiPSCs were positive for TRA-1-60, TRA-1-81, SOX 2, OCT4, and SSEA-4 in confocal immunofluorescence and positive for alkaline phosphatase in immunohistochemistry (representative pictures of three independent experiments). **c**, wt hiPSCs expressed typical pluripotency genes (representative gel of two independent PCR experiments). **d**, *B2M*$^{-/-}$*CIITA*$^{-/-}$ *CD47* tg hiPSCs maintained the normal human 46, XX karyotype in one analysis. **e**, *B2M*$^{-/-}$*CIITA*$^{-/-}$ *CD47* tg hiPSCs were also positive for TRA-1-60, TRA-1-81, SOX 2, OCT4, and SSEA-4 in confocal immunofluorescence and positive for alkaline phosphatase in immunohistochemistry (representative pictures of three independent experiments). **f**, *B2M*$^{-/-}$*CIITA*$^{-/-}$ *CD47* tg hiPSCs continued to express the typical pluripotency genes (representative gel of two independent PCR experiments). **g-j**, wt hiPSCs (g, h) and B2M-/- CIITA-/- CD47 tg hiPSCs (i, j) gave rise to cell types of all 3 germ layers after transplantation into SCID-beige mice. Endodermal (cytokeratin 8), mesodermal (brachyury), and ectodermal lineages (GFAP) were also demonstrated by confocal immunofluorescence microscopy (representative pictures of three independent experiments).

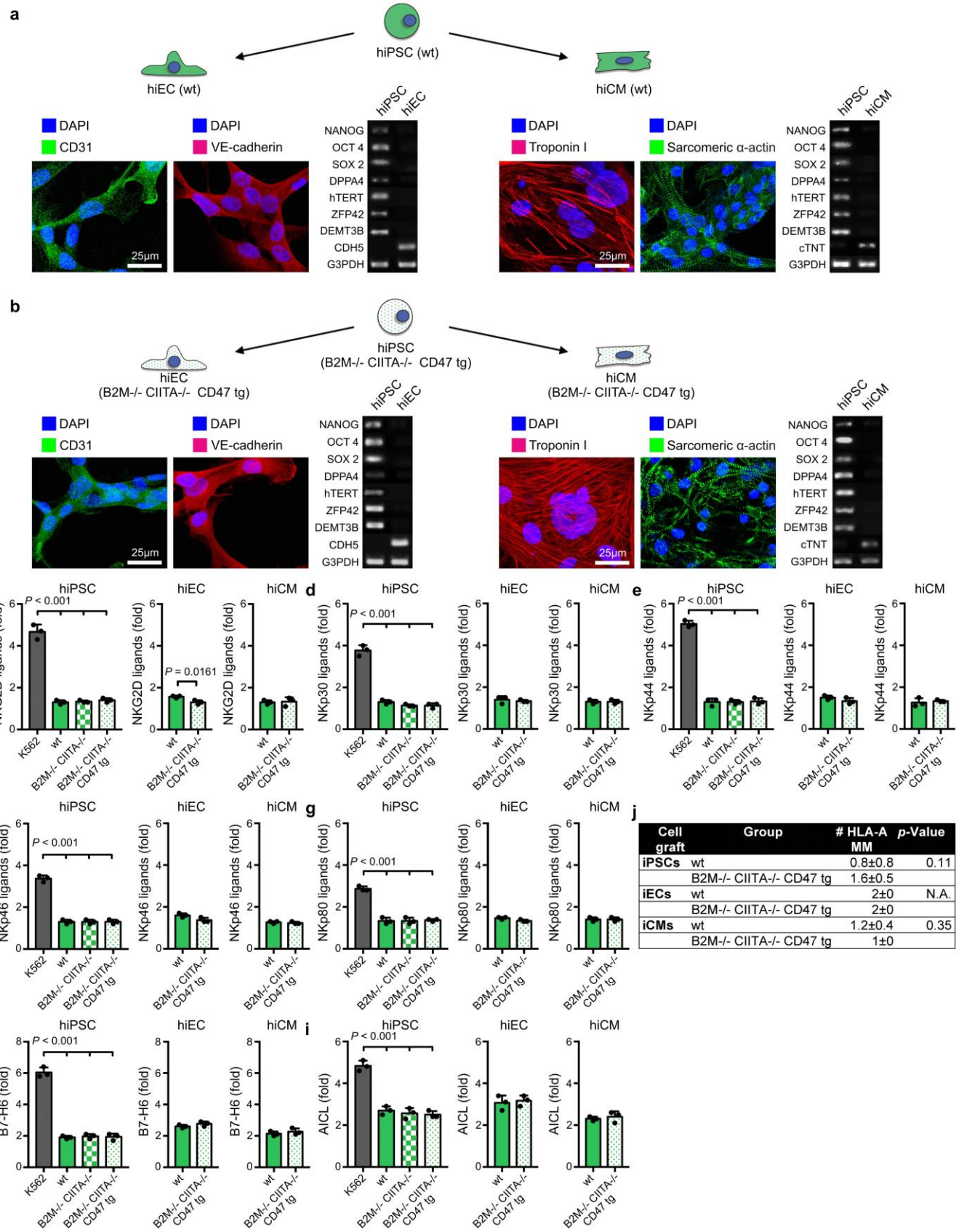

j

Cell graft	Group	# HLA-A MM	*p*-Value
iPSCs	wt	0.8±0.8	0.11
	B2M-/- CIITA-/- CD47 tg	1.6±0.5	
iECs	wt	2±0	N.A.
	B2M-/- CIITA-/- CD47 tg	2±0	
iCMs	wt	1.2±0.4	0.35
	B2M-/- CIITA-/- CD47 tg	1±0	

Supplementary Figure 12

Differentiation of hiPSCs into hiECs and hiCMs.

a-b, wt hiPSCs (a) and *B2M*$^{-/-}$*CIITA*$^{-/-}$ *CD47* tg hiPSCs (b) were successfully differentiated into corresponding miEC and miCM derivatives (representative pictures of three independent experiments). miECs were positive for CD31 and VE-cadherin and miCMs were positive for Troponin I and Sarcomeric alpha-actinin by confocal immunofluorescence. All derivatives lost their expression of pluripotency genes (representative pictures of two independent experiments). **c-g**, The expression of stimulatory NK cell ligands was assessed on hiPSCs and their derivatives using receptor Fc chimera proteins in flow cytometry (mean ± s.d., 3 independent experiments per group, ANOVA with Bonferroni's post-hoc test (hiPSCs) or two-tailed Student's t-test (hiECs and hiCMs)). Ligands for NKG2D (c), NKp30 (d), NKp44 (e), NKp46 (f), and NKp80 (g) were compared between wt and engineered hiPSCs, hiECs, hiCMs, and K562. **h-i**, The expression of specific human natural cytotoxicity receptor ligands was evaluated by flow cytometry (mean ± s.d., 3 independent experiments per group, ANOVA with Bonferroni's post-hoc test (hiPSCs) or two-tailed Student's t-test (hiECs and hiCMs)). Surface expression of B7-H6 (h), and AICL (i) was compared between wt and engineered hiPSCs and derivatives, and K562. **j**, The HLA-A mismatches in transplant experiments with wt and *B2M*$^{-/-}$*CIITA*$^{-/-}$ *CD47* tg hiPSCs, hiECs, and hiCMs in allogeneic humanized NSG-HGM3 recipients (mean ± s.d., 5 animals per group, two-tailed Student's t-test).

a

Assay	Cell graft	Group	CD3% of hCD45	*p*-Value
Elispot	iPSCs	wt	38±35	0.31
		B2M-/- CIITA-/- CD47 tg	57±31	
	iECs	wt	22±13	0.22
		B2M-/- CIITA-/- CD47 tg	63±48	
	iCMs	wt	25±22	0.96
		B2M-/- CIITA-/- CD47 tg	26±29	
BLI	iPSCs	wt	17±10	0.19
		B2M-/- CIITA-/- CD47 tg	38±32	
	iECs	wt	52±28	0.25
		B2M-/- CIITA-/- CD47 tg	34±18	
	iCMs	wt	18±12	0.56
		B2M-/- CIITA-/- CD47 tg	15±3	

c

Assay	Cell graft	Group	CD3% of hCD45	*p*-Value
Elispot	iECs	wt	48±18	0.70
		B2M-/- CIITA-/- CD47 tg	53±16	
BLI	iECs	wt	57±9	0.95
		B2M-/- CIITA-/- CD47 tg	58±8	

b

Experiments with NSG-SGM3 mice				
Assay	Group	Recipient HLA-A		# HLA-A MM to cell graft
Elispot iPSCs	wt	A*03:01	A*68:01	2
	wt	A*03:01	A*68:01	2
	wt	A*24:02	A*32:01	2
	wt	A*24:02	A*32:01	2
	wt	A*01:01	A*32:01	1
	wt	A*01:01	A*32:01	1
	wt	A*01:01	A*32:01	1
	B2M-/- CIITA-/- CD47 tg	A*03:01	A*68:01	2
	B2M-/- CIITA-/- CD47 tg	A*02:01	A*29:02	2
	B2M-/- CIITA-/- CD47 tg	A*24:02	A*32:01	2
	B2M-/- CIITA-/- CD47 tg	A*24:02	A*32:01	2
	B2M-/- CIITA-/- CD47 tg	A*01:01	A*30:02	1
	B2M-/- CIITA-/- CD47 tg	A*01:01	A*30:02	1
	B2M-/- CIITA-/- CD47 tg	A*32:01	A*66:01	2
Elispot CMs	wt	A*24:02	A*32:01	2
	wt	A*01:01	A*32:01	1
	wt	A*01:01	A*32:01	1
	B2M-/- CIITA-/- CD47 tg	A*24:02	A*32:01	2
	B2M-/- CIITA-/- CD47 tg	A*01:01	A*32:01	1
	B2M-/- CIITA-/- CD47 tg	A*01:01	A*32:01	1
Elispot Ecs	wt	A*24:02	A*25:01	2
	wt	A*24:02	A*25:01	2
	wt	A*24:02	A*25:01	2
	B2M-/- CIITA-/- CD47 tg	A*24:02	A*25:01	2
	B2M-/- CIITA-/- CD47 tg	A*03:01	A*68:01	2
	B2M-/- CIITA-/- CD47 tg	A*11:01	A*23:01	2
BLI_iPSC	wt	A*01:01	A*02:01	0
	wt	A*01:01	A*02:01	0
	wt	A*02:01	A*24:02	1
	wt	A*02:01	A*24:02	1
	wt	A*30:01	A*30:02	2
	B2M-/- CIITA-/- CD47 tg	A*24:02	A*32:01	2
	B2M-/- CIITA-/- CD47 tg	A*01:01	A*32:01	1
	B2M-/- CIITA-/- CD47 tg	A*01:01	A*32:01	1
	B2M-/- CIITA-/- CD47 tg	A*11:01	A*25:01	2
	B2M-/- CIITA-/- CD47 tg	A*11:01	A*25:01	2
BLI_EC	wt	A*11:01	A*25:01	2
	wt	A*11:01	A*25:01	2
	wt	A*11:01	A*25:01	2
	wt	A*11:01	A*25:01	2
	wt	A*11:01	A*25:01	2
	B2M-/- CIITA-/- CD47 tg	A*11:01	A*25:01	2
	B2M-/- CIITA-/- CD47 tg	A*11:01	A*25:01	2
	B2M-/- CIITA-/- CD47 tg	A*11:01	A*25:01	2
	B2M-/- CIITA-/- CD47 tg	A*11:01	A*25:01	2
	B2M-/- CIITA-/- CD47 tg	A*11:01	A*25:01	2
BLI_CM	wt	A*24:02	A*32:01	2
	wt	A*01:01	A*32:01	1
	wt	A*01:01	A*03:01	1
	wt	A*01:01	A*03:01	1
	wt	A*01:01	A*03:01	1
	B2M-/- CIITA-/- CD47 tg	A*01:01	A*03:01	1
	B2M-/- CIITA-/- CD47 tg	A*01:01	A*03:01	1
	B2M-/- CIITA-/- CD47 tg	A*01:01	A*03:01	1
	B2M-/- CIITA-/- CD47 tg	A*01:01	A*03:01	1
	B2M-/- CIITA-/- CD47 tg	A*01:01	A*03:01	1

Supplementary Figure 13

CD3 reconstitution and HLA matching in humanized mice.

a, Percentage of $CD3^+$ cells among the reconstituted human $CD45^+$ cell population in NSG-SGM3 mice receiving hiPSC grafts (n=7 per group), hiEC grafts (n=3 per group), or hiCM grafts (n=3 per group) in the Elispot groups or hiPSC grafts, hiEC grafts, or hiCM grafts (n=5 per group) in the BLI groups (mean ± s.d., two-tailed Student's t-test). **b**, All NSG-SGM3 mice were typed for HLA-A and the number of HLA-A mismatches (MM) was calculated for every single animal used in this study. 2 MM are coded in red, 1 MM in orange, and zero MM in green. **c**, Percentage of $CD3^+$ cells among the reconstituted human $CD45^+$ cell population in BLT mice receiving iEC grafts in the Elispot groups (n=4 per group) or BLI groups (n=5) (mean ± s.d., two-tailed Student's t-test).